Antiangiogenic properties of fibstatin, an extracellular FGF-2-binding polypeptide.

Carine Bossard, Loic van den Berghe, Henrik Laurell, Caroline Castano, Martine Cerutti, Anne-Catherine Prats, Hervé Prats

Antiangiogenic properties of Fibstatin, an extracellular FGF-2 binding polypeptide [1]

Carine Bossard [2], Loic Van den Berghe, Henrik Laurell, Caroline Castano, Martine Cerutti, Anne-Catherine Prats and Hervé Prats [3].

INSERM U589, C.H.U. Rangueil, 31403 Toulouse Cedex 04, France [C.B., L.V., H.L., AC.P., H.P.] and INRA - CNRS UMR 5087 30380 Saint Christol Lès Alès, France [M.C.].

Running title: Fibstatin, an antiangiogenic FGF-binding peptide

Key words: anti-angiogenesis, FGF-2, Fibronectin, tumor inhibition

[1] Supported by grants from INSERM, University Paul Sabatier Toulouse, la Ligue Contre le Cancer, Conseil Régional Midi-Pyrénées, European Commission FP5 (QOL-2000-3.1.2, consortium CONTEXTH contract QLRT-2000-00721) and the French Ministery of Research (decision No 01H0387).

[2] Supported by the Association pour la Recherche contre le Cancer.

[3] To whom requests for reprints should be addressed at U589, CHU Rangueil, Bat L3, 31403 Toulouse cedex 4, tel: (33) 561 322 144, fax: (33) 561 322 141, e-mail: pratsh@toulouse.inserm.fr

Abstract

By using the two-hybrid system with FGF-2 (basic Fibroblast Growth Factor) as bait, we isolated and characterized an endogenous 29 kDa human basement membrane-derived inhibitor of angiogenesis and tumor growth, we termed Fibstatin. Fibstatin, a fragment containing the type III domains 12-14 of Fibronectin, was produced as a recombinant protein and was shown to inhibit the proliferation, migration and differentiation of endothelial cells *in vitro*. Anti-angiogenic activity of Fibstatin was confirmed in a Matrigel angiogenesis assay *in vivo* and electrotransfer of the Fibstatin gene into muscle tissue resulted in reduced B16F10 tumor growth. Taken together, these results suggest that Fibstatin could act as a powerful molecule for anti-angiogenic therapy.

INTRODUCTION

Angiogenesis, the outgrowth of new capillaries from pre-existing vessels, is not only essential for a number of physiological processes but also occurs in many pathological conditions including tumor growth. This phenomenon is tightly controlled by numerous angiogenic factors whose effects are counterbalanced by inhibitory molecules such as Endostatin and Angiostatin which are proteolytic polypeptides derived from collagen XVIII and plasminogen, respectively (1, 2). Among the angiogenic growth factors, FGF-2 is one of the most efficient (3).

It can exert its activity both as an endogenous (intracrine) and an exogenous (auto-/paracrine) factor through different pathways. Exogenous FGF2 act via cell surface receptors linked to conventional signal transduction pathways, but also through direct association with the nuclei of target cells after internalisation and nuclear translocation during the G1 phase of the cell cycle (4). We have recently shown that this nuclear translocation is necessary for the mitogenic activity of FGF-2 and is mediated by Translokin, isolated by the two-hybrid system with FGF-2 18 kDa as bait (5).

In the same screening, we isolated two independent clones encoding fragments of Fibronectin that also showed a strong interaction with FGF-2. It has been previously reported that the amino- and carboxy-terminal heparin–binding domain of human plasma Fibronectin appear to be rather specific potent inhibitors of bovine aortic endothelial cell growth in culture by an unknown mechanism, whereas the plasma Fibronectin itself is much less inhibitory (6). We thus evaluated whether the shortest of the two FGF-2 interacting fragments could counteract the angiogenic properties of FGF-2. Given its anti-angiogenic activity we named the fragment Fibstatin.

Because angiogenesis represents a cascade of cellular processes that includes endothelial cell proliferation, migration and tube formation (7), we used multiple *in vitro* and *in vivo* assays related to angiogenesis to confirm the bioactivity of Fibstatin.

MATERIALS AND METHODS

Yeast two-hybrid system

The two-hybrid expression-cloning system was carried out as described by Van den Berghe *et al.* (8). Briefly, the 18 kDa FGF-2 was used as bait, and the corresponding cDNA was inserted in the pAS2 vector. A human placenta library (Clontech, Palo Alto, CA) cloned into the pACT2 vector was screened in *Saccharomyces cerevisiae* strain Y190. ß-galactosidase activity of colonies growing on selection medium (DOB-Arg/-Trp/-Leu) was assessed by blue/white coloring (X-gal assay) and in yeast extracts using Galacto-Light (Tropix Inc. Bedford, MA) as described by the manufacturer. The activity was normalized for protein contents.

Plasmids encoding Fibstatin or Endostatin

The coding sequence of Fibstatin was amplified by PCR from the pACT2 plasmid containing the Fibstatin cDNA isolated by the two hybrid screening. The coding sequence of Endostatin was amplified by RT-PCR from RNA extracted from NIH-3T3 cells. The two cDNAs were then ligated into pET-15b (Novagen, Madison, WI) in frame with the histidine tag for recombinant protein production in *E.coli* or cloned in the eukaryotic expression vectors, pUHD10-3 (9) and pSCT (10) in frame with the signal peptide of VEGF-A (11) and the HA epitope, for use in conditioned media preparation and electrotransfer, respectively. For the structure-functional analysis of the FGF2-Fibstatin complex, given regions of Fibstatin were amplified by PCR, respecting the limits of each type III module (Fig. 1). The amplified products were cloned in frame with the transactivating domain of Gal4 in pACT2 vector. All the sequences were confirmed by automatic sequencing using the ABI Prism Dye

Terminator kit (Applied Biosystems, Foster City, CA). Cloning details can be provided upon request.

Recombinant protein expression

Using E.coli BL21 (DE3). The production and purification of recombinant proteins were performed with Ni^{2+}-NTA beads (Qiagen, Courtaboeuf, France) as described by Holzinger et *al.* (12).

Using Baculovirus. The coding sequences for Fibstatin and Endostatin were subcloned into the transfer vector p119 designed for recombination in the P10 locus as described by Marchal et al. (13). Briefly, by using DOTAP (Roche), Sf9 cells were cotransfected with p119-Fib or p119-Endo and purified viral DNA of baculovirus AcSLP10 expressing the polyhedrin gene under the control of the P10 promoter (14). The screening and purification of the recombinant virus were carried out as reported by Summers and Smith (15). Fibstatin and Endostatin were purified from the serum-free supernatant of Sf9 cells. The supernatant (1 liter) was slowly mixed with ammonium sulfate to obtain a final concentration of 50%. The ammonium sulfate/supernatant solution was stirred 2 hours at 4°C and centrifuged at 5000 rpm for 30 min. The precipitated proteins were resuspended in 0.1 starting volumes of PBS. The solution was dialyzed against PBS and the proteins were purified by using Ni^{2+}-NTA beads according to the manufacturer (Qiagen).

Cell culture

NIH-3T3, HeLa HT (16) and ABAE cells were grown in DMEM (Invitrogen, Cergy Pontoise, France) containing antibiotics, 1% glutamine and 10 % fetal calf serum (FCS) or 10% calf serum (CS) for ABAE. B16F10 cells were grown in RPMI 1640

(Biowhittaker, Emerainville, France) containing antibiotics, 1% glutamine and 10 % FCS. Cells were maintained in a 37°C and 10% CO_2 (for ABAE) or 5% CO_2 (for NIH-3T3, HeLa and B16F10 cells) humidified incubator.

***In vitro* transfection and conditioned media preparation**

HeLa HT cells seeded at $1.2x10^6$ per 100 mm tissue culture dish were transfected with 17 µg of plasmid pUHD-Fibstatin, pUHD-Endostatin or "empty" pUHD by using Fugene 6 reagent according to the manufacturer's recommendations (Roche Diagnostics, Mannheim, Germany). Twenty-four hours after the transfection, subconfluent cells were washed with DMEM and incubated in DMEM supplemented with 1% FCS. Twenty-four hours later, cell-conditioned medium was collected, centrifuged to remove cell debris and stored at –80°C until use.

Proliferation assay

Using conditioned medium. ABAE cells were seeded at $5x10^4$/ml of medium. Twenty-four hours later, cells were washed with DMEM and incubated with different dilutions of transfected-HeLa cells conditioned medium so that the final calf serum concentration was 10%. The proliferation was stimulated with 0.5 ng/ml FGF-2. The media was changed twice and after 72 h, cells were counted with a Coulter counter ZM (Beckman Coulter, Villepinte, France).

Using recombinant protein. ABAE cells seeded at $5x10^3$/ml were stimulated by 0.5 ng/ml FGF-2 with different concentrations of Fibstatin or Endostatin added at day 1 and 3. At day 5 cells were trypsinized and counted with a Coulter counter ZM.

Cell migration assay

ABAE cells were grown to confluence in complete medium. The cells were then incubated in serum-free DMEM for 48h prior to the experiment. A scratch injury was applied on the cell monolayer using a plastic pipette tip to generate a wound. The debris were removed by washing the cells with PBS, and the cells were incubated for 14 h in serum-free DMEM supplemented with FGF-2 (3 ng/ml) in the presence or not (control) of Fibstatin (1µg/ml). Migrating cells were then counted under microscope.

***In vitro* angiogenesis assay**

Twenty-four-well plates were coated with 300 µl Growth Factor Reduced Matrigel™ (B&D, Bedford, MA) per well, which was allowed to polymerize for 1h at 37°C. ABAE cells ($2x10^5$ cells/ml) suspended in 500 µl of culture medium were then added to each well. FGF-2 (0.5 ng/ml) with or without (control) Fibstatin (1µg/ml) was added to the wells and the plates were incubated overnight at 37°C. After removal of the medium, the culture was fixed and the length of the tube network was quantified with the Q Win Leica system (Leica Microsystems, Rueil-Malmaison, France).

Animals studies

Six-to 10-week-old C57Bl/6 mice were housed in stainless-steel cages in groups of 5, kept in a temperature-controlled facility on a 12-h light-dark cycle, and fed normal laboratory mouse chow diet. All procedures were performed in accordance with the recommendations of the European Accreditation of Laboratory Animal Care.

***In vivo* angiogenesis assay**

8 to 10 week-old C57Bl/6 female mice received a subcutaneous injection (0.3 ml) of Growth Factor Reduced Phenol-red-free Matrigel (BD Biosciences, Bedford, MA) supplemented with FGF-2 (100 ng/ml) alone (control) or in the presence of Fibstatin or Endostatin (10 μg/ml). Matrigel plugs were removed 7 days later, weighed and dissolved in 1.5 ml of Matrisperse™ cell release solution (BD Biosciences) during two hours at 4°C. After dispersion from the gel, microvascular endothelial cells were counted under a microscope with a Malassez cell, and the cell number was normalized or not by the weight of the Matrigel. The phenotype of the cells was verified by the staining with anti-CD31 (Pharmingen, San Diego, CA).

Electrotransfer of plasmid encoding Fibstatin or Endostatin into quadriceps of mice bearing B16F10 melanoma

Fifteen mice were used in each control or experimental group. The mice were anesthesized with ketamin (150 mg/kg) and subjected to a dorsal subcutanous injection of $1x10^6$ B16F10 cells in 100 μl PBS^- (i.e. standard PBS without Ca^{2+} and Mg^{2+}). At the same time, 50 μg of pSCT DNA plasmid, encoding or not Fibstatin (pSCT Fib) or Endostatin (pSCT Endo), were mixed with 5 μg of DNA plasmid encoding the β-Galactosidase, and injected in 50 μl of PBS^- into the quadriceps. Only endotoxin-free plasmids were used (Endofree Plasmid Maxi Kit; Qiagen). The quadriceps were then entirely covered with ultrasound gel and placed between 10 mm diameter caliper-type electrodes set 4 mm apart, and electroporated with 8 pulses (80 V, 20 milliseconds) from an ElectroSquare Porator ECM830 (BTX, a division of Genetronics, San Diego, CA). Electroporation was repeated 5 days later. Tumors were excised and weighed 10 days after the first injection. $P<0.05$ was considered as

statistically significant using a one-factor ANOVA. Endostatin concentration was assayed by Elisa (Accucyte Murine Endostatin Immunoassay Kit; Cytimmune Science, College Park, MD). For determination of β-Galactosidase activity, the electroporated quadriceps were excised and placed in 350 µl of β-Gal lysis solution (Tropix, Bedford, MA) and homogenized. The homogenate was centrifuged (13,000 rpm, 10 minutes) and 20 µl of supernatant was used to measure the β-Galactosidase activity using the commercial kit Galacto Light (Tropix, Bedford, MA).

CD31 Immunostaining

Intratumoral microvessel density was analyzed on frozen sections (5 µm) of B16 melanoma using a rat anti-mouse CD31 monoclonal antibody (Pharmingen, San Diego, CA). After fixation in 4% paraformaldehyde for 1h at 4°C, the sections were washed 3 times with PBS and were permeabilized using PBS-0.25% Triton X100-3% BSA for 1h. After blocking with 5% rabbit serum/PBS-Tween 0.1% for 1h at room temperature, the sections were incubated overnight with the anti-mouse CD31 antibody, diluted 1:50 in antibody diluent solution (DAKO, Carpinteria, CA). The sections were washed three times with PBS and incubated with biotinylated anti rat IgG (Vector Labs, Burlingame, CA) diluted 1:200 in antibody diluent solution during 2h at room temperature. After three washings with PBS, a Streptavidin Alexa Fluor 488 conjugate (Molecular probes, Eugene, OR) diluted 1:200 in antibody diluant solution was used for detection of bound antibodies. The Visiolab 2000 software (Biocom, Paris, France) was used to quantify the anti-CD31 labeled surface.

RESULTS

Isolation of a novel FGF-2 interacting protein

In a two-hybrid screening, we isolated two independent clones that interacted strongly with FGF-2 (Fig. 1*A*). These two clones named A and B, contain the heparin binding domain 2 (hep2) of Fibronectin and mainly differ in the length of their NH2 extremities (Fig. 1*B*). After a more substantial characterization of the properties of the shortest clone B (see below), which overlaps with the three type III modules (FNIII 12-14) of Fibronectin, we named the corresponding peptide Fibstatin.

To test the specificity of the observed interaction between Fibstatin and FGF-2, we coexpressed Fibstatin in yeast with a panel of representative FGF-family members (FGF-1, FGF-3, FGF-6, FGF-12). Among the FGFs tested, only FGF-2 was able to interact with Fibstatin (Fig. 2*A*). To ascertain that the Fibstatin/FGF-2 interaction was direct and independent of a third partner, we expressed the two proteins in *E.coli*, purified them and tested their interaction in an *in vitro* ELISA assay as described by Bossard et al. (5). Fibstatin and FGF-2 interact strongly in a direct and dose-dependent manner (Fig. 2*B*). We next determined which of the three type III modules (FNIII 12-14) in Fibstatin that contains the FGF-2 interacting site. Different portions of Fibstatin were subcloned in pACT2 and their capacity to interact with FGF-2 was tested in the two-hybrid system. We found that both FNIII 13 and 14 are necessary to maintain a similar level of binding as full length Fibstatin (Fig. 2*C*). When tested separately, the two modules were not able to interact with FGF-2, except for a residual interaction (10%) for FNIII 14. These results suggest that two structural motifs in Fibstatin, the type III modules 13 and 14, cooperate in the binding to FGF-2.

Fibstatin inhibits endothelial cells proliferation

Since FGF-2 is a strong inducer of endothelial cell proliferation, Fibstatin was tested for its activity on FGF-2-induced proliferation of ABAE cells and compared with the inhibitory activity of Endostatin. For this purpose, we prepared conditioned media from transiently transfected HeLa HT. The presence of Fibstatin or Endostatin, which have an apparent molecular weight of 29 kDa and 20 kDa, respectively, was confirmed by SDS-PAGE (data not shown). The conditioned media were then applied at different dilutions to FGF-2-stimulated ABAE cells, in a 72 h proliferation assay. Fibstatin and Endostatin expressed in the conditioned media inhibited in a dose-dependent manner the ABAE proliferation induced by FGF-2 (Fig. 3*A*). A similar inhibitory effect on ABAE cells was observed when recombinant Fibstatin produced in *E.coli* was used in the above assay (Fig. 3*B*). Interestingly, the inhibitory effect of Fibstatin was greater compared to that of Endostatin, at every dose tested. On the contrary, no significant inhibition of proliferation was observed when cells of nonendothelial origin, such as fibroblasts NIH-3T3 or B16F10, were tested (Fig. 3*C*).

Fibstatin inhibits endothelial cells migration and tubulogenesis

To test the ability of recombinant Fibstatin to inhibit endothelial cell migration induced by FGF-2, we used an *in vitro* wounding assay. The addition of 1 μg/ml Fibstatin greatly reduced the number of migrating ABAE cells upon FGF-2 stimulation (Fig. 4*A*). To determine the *in vitro* antiangiogenic effects of Fibstatin, we tested its ability to interfere with endothelial cell tube formation in Matrigel, a solid gel of basement membrane proteins derived from mouse sarcoma. When FGF-2 stimulated ABAE cells were cultured on Matrigel, they rapidly aligned and formed

hollow tube-like structures. In the presence of Fibstatin produced in *E.coli*, the tube formation induced by FGF-2 was inhibited and the cells appeared clustered, as in the absence of FGF-2 (Fig. 4*B*).

In vivo antiangiogenic activities of Fibstatin

We then tested the ability of recombinant Fibstatin to inhibit *in vivo* angiogenesis. For this purpose, Matrigel plugs containing FGF-2 with or without baculovirus-expressed Fibstatin or Endostatin were injected subcutaneously in C57Bl/6 mice. One week after implant, the endothelial cells having colonized the plugs were counted. Under these conditions, more than 90% of the cells in the Matrigel are positive for the endothelial marker CD 31 (data not shown). The number of cells within the plugs containing both FGF-2 and Fibstatin was 50% compared with the control containing only FGF-2. Interestingly, Fibstatin was more potent than Endostatin in inhibiting the angiogenic activity of FGF-2 (Fig. 5*A*). One could argue that this result is due to an effect of Fibstatin on matrix degrading protease, provoking matrigel degradation and the apparent decrease in cell number per unit matrigel weight. We then considered the cell numbers without normalizing them. As shown in Fig. 4*A*, even if the inhibition is lower in this condition (40%), it is still significant, consistent with an antiangiogenic activity of Fibstatin.

Electrotransfer of Fibstatin-encoding cDNA into muscles inhibits B16F10 tumor growth

We then evaluated the *in vivo* effect of Fibstatin on tumor growth after DNA electrotransfer. Fibstatin- or Endostatin-encoding plasmid DNA were mixed with a reporter plasmid encoding LacZ, injected and electroporated into quadriceps of

C57Bl/6 mice, previously inoculated with B16F10 cells. The electroporation was repeated 5 days later. In the group of mice treated with the Fibstatin-coding gene, there was a 50% inhibition of tumor growth compared to control mice injected with empty vector. This inhibition was observed at day 10 (Fig. 5*B*) and also at day 14 (data not shown). Tumor mass in the Endostatin-treated group was reduced, but the difference did not reach statistical significance (Fig. 5*B*). To assess the efficiency of the gene transfer, the β-galactosidase activity was measured in muscle lysate. The results, shown in Fig. 5*C*, reveal a significant β-galactosidase activity in all electroporated mice.

The circulating Endostatin level was determined by the use of a commercially available ELISA kit. Endostatin level in the blood of mice electrotransferred with a plasmid encoding Endostatin was markedly higher than in the blood of control mice (Fig. 5*D*). In order to detect the level of circulating Fibstatin, we developed a rabbit polyclonal antibody which specifically recognizes the protein but was insufficient to detect low concentrations of the protein (data not shown). Even though we were unable to quantify the amount of circulating Fibstatin, the efficiency of the electrotransfer was ascertained by the quantification of the ß-Galactosidase activity in the transfected muscles (Fig. 5*C*). Moreover, the transgene expression from both plasmids is similar when transfected in mammalian cells (data not shown).

Fibstatin inhibits tumor angiogenesis

To elucidate whether the effect of Fibstatin gene delivery on melanoma growth was due to an inhibition of angiogenesis, tumor capillaries were examined by anti-CD31 immunostaining. As shown in Fig. 6, representative tumor sections from Fibstatin and Endostatin treated mice showed a significant decrease in CD31 staining, compared to

the tumor sections from control mice. Quantification of microvessels at 200 fold magnification indicated that the CD31 positive surface in tumors from control mice was 2.2% ± 0,58 (mean±SD), compared to 0.74% ± 0.23 and 0.94% ± 0.39 in Fibstatin and Endostatin treated tumors, respectively (Fig. 6*B*). Taken together, these data demonstrate that Fibstatin gene delivery inhibits the angiogenic response *in vivo* in a B16-F10 melanoma immunocompetent mouse model.

Discussion

In this paper we report the identification of Fibstatin, a human Fibronectin fragment that interacts specifically with FGF-2 and corresponds to the major heparin binding domain (hep2) of Fibronectin. Interestingly, Fibstatin is highly similar to the 29 kDa fragment which is generated when Fibronectin is digested by Dispase (17). This indicates that such a fragment could be produced in physio(patho)logical conditions. Here we demonstrate that Fibstatin functions as an anti-angiogenic molecule that inhibits *in vitro* FGF-2 dependent proliferation, migration and tube formation of endothelial cells. This may indicate that, similar to FGF-2, Fibstatin interferes with more than one step in the angiogenic process. *In vivo,* Fibstatin inhibits Matrigel neovascularization and the growth of B16F10 melanoma. Tumor angiogenesis in melanoma was examined using CD31 immunostaining. Our results show a rarefaction of small blood vessels in both Fibstatin and Endostatin treated tumor tissue sections as compared with the control, indicating a role of Fibstatin in suppressing tumor angiogenesis. Since Fibstatin did not show any *in vitro* activity on the proliferation of B16F10 cells, its inhibitory effects on tumor growth is likely due to its antiangiogenic properties. To evaluate the antiangiogenic activities of Fibstatin, we made a comparison with Endostatin, one of the most described antiangiogenic factor. In our study, Fibstatin is more efficient than Endostatin when used as recombinant protein. However, the activity of Endostatin is sensitive on its interaction with zinc (18). The results obtained with recombinant protein show that the effect of Fibstatin is always efficient, independently of its mode of preparation. The process of protein purification may denature the Endostatin protein and yield rates may be low. Gene delivery should in theory abrogate this problem (19). Moreover, because angiostatic therapy would

require a prolonged maintenance of therapeutic levels *in vivo*, the continuous delivery of a recombinant protein would be expensive and cumbersome. *In vivo* transfer of the corresponding genes constitutes an attractive solution to this problem.

For this reason, we evaluated the respective effect of Endostatin and Fibstatin on tumor growth after gene delivery. In this experiment, the anti-tumorigenic effect of Fibstatin is still more powerful than the effect of Endostatin.

The high affinity for heparin by both Fibstatin and FGF-2 rises the question whether heparin acts as a mediator in the interaction between Fibstatin and FGF-2. Our results indicate that this interaction could be independent of the heparin binding of Fibstatin since the interaction occurs *in vitro* between recombinant proteins without any addition of heparin or heparan sulfates proteoglycans (HSPG). Fibstatin could interact directly with FGF-2 and thus inhibits, like PF-4 or Thrombospondin, the interaction between FGF-2 and its receptors, or the dimerization or internalization of the growth factor (20, 21). Furthermore we have mapped the Fibronectin modules which are required for the binding with FGF-2. The module 13 plays a major role in the interaction with heparin (22, 23). However, this module alone is unable to interact with FGF-2. Indeed, both modules 13 and 14 are required for an efficient binding of FGF-2. Nevertheless, most of the endogenous antiangiogenic proteins identified so far, like Endostatin, Angiostatin, PF-4 and Kallistatin bind to heparin (1, 2, 6, 24, 25). This property is collectively interpreted as involved in the inhibition of FGF/VEGF activity by competing for their interaction with HSPG. Indeed, these two angiogenic factors present a strong heparin binding activity.

It thus appears that at least two modes of action could be invoked for Fibstatin: the binding to HSPG and the direct protein-protein interaction with FGF-2. In addition, we could also speculate that Fibstatin acts by binding to integrins. Indeed Fibstatin

corresponds to the 12-14 type III domain, which binds to $\alpha_{IIb}\beta_3$ (26) and $\alpha_4\beta_1$ (27). Moreover, it has been recently shown that two other antiangiogenic factors, Tumstatin and Endostatin, exhibit their activities through $\alpha_v\beta_3$ and $\alpha_5\beta_1$ integrins (28).

The characterization of novel antiangiogenic proteins and the elucidation of their mode of action is of great importance. Indeed, it would allow to consider associative strategies by using electrotransfer of polycistronic vectors expressing in the same time several antiangiogenic peptides with different properties in order to obtain an optimal angiogenesis inhibition.

Acknowledgements

We thank Alexia Schambourg, Catherine Zanibellato, Marcel Mariller and Annick Ozil for technical assistance.

References :

1. O'Reilly, M. S., Boehm, T., Shing, Y., Fukai, N., Vasios, G., Lane, W. S., Flynn, E., Birkhead, J. R., Olsen, B. R., and Folkman, J. Endostatin: an endogenous inhibitor of angiogenesis and tumor growth. Cell, *88:* 277-285., 1997.
2. O'Reilly, M. S., Holmgren, L., Shing, Y., Chen, C., Rosenthal, R. A., Moses, M., Lane, W. S., Cao, Y., Sage, E. H., and Folkman, J. Angiostatin: a novel angiogenesis inhibitor that mediates the suppression of metastases by a Lewis lung carcinoma. Cell, *79:* 315-328., 1994.
3. Bikfalvi, A., Klein, S., Pintucci, G., and Rifkin, D. B. Biological roles of fibroblast growth factor-2. Endocr Rev, *18:* 26-45, 1997.
4. Baldin, V., Roman, A. M., Bosc-Bierne, I., Amalric, F., and Bouche, G. Translocation of bFGF to the nucleus is G1 phase cell cycle specific in bovine aortic endothelial cells. Embo J, *9:* 1511-1517., 1990.
5. Bossard, C., Laurell, H., Van Den Berghe, L., Meunier, S., Zanibellato, C., and Prats, H. Translokin is an intracellular mediator of FGF-2 trafficking. Nat Cell Biol, *5:* 433-439., 2003.
6. Homandberg, G. A., Williams, J. E., Grant, D., Schumacher, B., and Eisenstein, R. Heparin-binding fragments of fibronectin are potent inhibitors of endothelial cell growth. Am J Pathol, *120:* 327-332., 1985.

7. Folkman, J. and Shing, Y. Angiogenesis. J Biol Chem, *267:* 10931-10934., 1992.

8. Van den Berghe, L., Laurell, H., Huez, I., Zanibellato, C., Prats, H., and Bugler, B. FIF [fibroblast growth factor-2 (FGF-2)-interacting-factor], a nuclear putatively antiapoptotic factor, interacts specifically with FGF-2. Mol Endocrinol, *14:* 1709-1724., 2000.

9. Gossen, M. and Bujard, H. Tight control of gene expression in mammalian cells by tetracycline- responsive promoters. Proc Natl Acad Sci U S A, *89:* 5547-5551, 1992.

10. Prats, A. C., Vagner, S., Prats, H., and Amalric, F. cis-acting elements involved in the alternative translation initiation process of human basic fibroblast growth factor mRNA. Mol Cell Biol, *12:* 4796-4805., 1992.

11. Huez, I., Bornes, S., Bresson, D., Creancier, L., and Prats, H. New vascular endothelial growth factor isoform generated by internal ribosome entry site-driven CUG translation initiation. Mol Endocrinol, *15:* 2197-2210., 2001.

12. Holzinger, A., Phillips, K. S., and Weaver, T. E. Single-step purification/solubilization of recombinant proteins: application to surfactant protein B. Biotechniques, *20:* 804-806, 808, 1996.

13. Marchal, I., Cerutti, M., Mir, A. M., Juliant, S., Devauchelle, G., Cacan, R., and Verbert, A. Expression of a membrane-bound form of Trypanosoma cruzi trans-sialidase in baculovirus-infected insect cells: a potential tool for sialylation of glycoproteins produced in the baculovirus-insect cells system. Glycobiology, *11:* 593-603, 2001.

14. Chaabihi, H., Ogliastro, M. H., Martin, M., Giraud, C., Devauchelle, G., and Cerutti, M. Competition between baculovirus polyhedrin and p10 gene expression during infection of insect cells. J Virol, *67:* 2664-2671, 1993.

15. Summers, M. and Smith, G. A Manual of Methods for Baculovirus Vectors and Insect Cell Culture Procedures. Texas Agricultural Experiment Station, College Station, TX., 1987.

16. Cayrol, C. and Flemington, E. K. Identification of cellular target genes of the Epstein-Barr virus transactivator Zta: activation of transforming growth factor beta igh3 (TGF-beta igh3) and TGF-beta 1. J Virol, *69:* 4206-4212, 1995.

17. Fujita, H., Mohri, H., Kanamori, H., Iwamatsu, A., and Okubo, T. Binding site in human plasma fibronectin to HL-60 cells localizes in the C-terminal heparin-binding region independently of RGD and CS1. Exp Cell Res, *217:* 484-489, 1995.

18. Boehm, T., O'Reilly M, S., Keough, K., Shiloach, J., Shapiro, R., and Folkman, J. Zinc-binding of endostatin is essential for its antiangiogenic activity. Biochem Biophys Res Commun, *252:* 190-194, 1998.

19. Wen, X. Y., Bai, Y., and Stewart, A. K. Adenovirus-mediated human endostatin gene delivery demonstrates strain-specific antitumor activity and acute dose-dependent toxicity in mice. Hum Gene Ther, *12:* 347-358, 2001.

20. Perollet, C., Han, Z. C., Savona, C., Caen, J. P., and Bikfalvi, A. Platelet factor 4 modulates fibroblast growth factor 2 (FGF-2) activity and inhibits FGF-2 dimerization. Blood, *91:* 3289-3299., 1998.

21. Taraboletti, G., Belotti, D., Borsotti, P., Vergani, V., Rusnati, M., Presta, M., and Giavazzi, R. The 140-kilodalton antiangiogenic fragment of

thrombospondin-1 binds to basic fibroblast growth factor. Cell Growth Differ, *8:* 471-479, 1997.

22. Sachchidanand, Lequin, O., Staunton, D., Mulloy, B., Forster, M. J., Yoshida, K., and Campbell, I. D. Mapping the heparin-binding site on the 13-14F3 fragment of fibronectin. J Biol Chem, *277:* 50629-50635, 2002.

23. Sharma, A., Askari, J. A., Humphries, M. J., Jones, E. Y., and Stuart, D. I. Crystal structure of a heparin- and integrin-binding segment of human fibronectin. Embo J, *18:* 1468-1479, 1999.

24. Levine, S. P. and Wohl, H. Human platelet factor 4: Purification and characterization by affinity chromatography. Purification of human platelet factor 4. J Biol Chem, *251:* 324-328., 1976.

25. Miao, R. Q., Agata, J., Chao, L., and Chao, J. Kallistatin is a new inhibitor of angiogenesis and tumor growth. Blood, *100:* 3245-3252, 2002.

26. Mohri, H., Tanabe, J., Katoh, K., and Okubo, T. Identification of a novel binding site to the integrin alphaIIbbeta3 located in the C-terminal heparin-binding domain of human plasma fibronectin. J Biol Chem, *271:* 15724-15728, 1996.

27. Mould, A. P. and Humphries, M. J. Identification of a novel recognition sequence for the integrin alpha 4 beta 1 in the COOH-terminal heparin-binding domain of fibronectin. Embo J, *10:* 4089-4095, 1991.

28. Sudhakar, A., Sugimoto, H., Yang, C., Lively, J., Zeisberg, M., and Kalluri, R. Human tumstatin and human endostatin exhibit distinct antiangiogenic activities mediated by alpha v beta 3 and alpha 5 beta 1 integrins. Proc Natl Acad Sci U S A, *100:* 4766-4771, 2003.

Figure Legends

Fig. 1 : Characterization of Fibstatin, an FGF-2 interacting protein

A, Domain structure of human Fibronectin and relative position of the two FGF-2 binding clones (A,B) isolated by the two-hybrid system. **B**, Amino acid sequence of the two FGF-2 binding clones (A,B). Arrows indicate the extremities of each clone. The type III(12) domain is in italics, the type III(13) domain is in bold and the type III(14) domain is underlined.

Fig. 2: Specific and direct interaction between Fibstatin and FGF-2

A, Specificity of the interaction between Fibstatin and FGF-2. Several FGFs and Fibstatin were fused to DNA binding (DB) or activating (AD) domains of Gal4 and subjected to a yeast two hybrid assay to evaluate the degree of interaction. **B,** Direct interaction between FGF-2 and Fibstatin by ELISA. FGF-2 and BSA were coated on a 96-well plate and incubated with different concentration of His-tagged recombinant Fibstatin. The association was revealed using a horse-radish-peroxidase-conjugated antibody against the $(His)_6$ tag, and quantified at 490 nm in an ELISA microplate reader. Binding was calculated by substraction of nonspecific binding obtained with BSA. Data are the mean ± S.D. of a representative triplicate samples. **C**, Analysis of structural elements of Fibstatin involved in the interaction with FGF-2. The capacity of modules type III 12-14, alone or together, to interact with FGF-2 was assessed in the yeast two-hybrid system. The bars indicate the β-galactosidase activity ± SD in yeast extracts from 3 independent transformations.

Fig. 3 : Fibstatin inhibits endothelial cells proliferation

A, Inhibition of bovine aortic endothelial cell proliferation by conditioned media from HeLa cells expressing or not (control) Fibstatin or Endostatin. Diluted conditioned media (one plus one volume (1:2) or three plus one volumes (3:4)), supplemented with serum and 0.5 ng/ml FGF-2, was applied to bovine aortic endothelial cells in a 72h proliferation assay. Data are expressed as % of the proliferation of FGF-2-stimulated control cells ± SD. **B**, Inhibition of aortic endothelial cell proliferation by recombinant Fibstatin or Endostatin. Different concentrations of recombinant Fibstatin or Endostatin were applied to ABAE cells stimulated with 0.5 ng/ml of FGF-2 at day 1 and 3. At day 5, cells were trypsinized and counted with a Coulter counter ZM. Data are expressed as % of the proliferation of FGF-2-stimulated control cells ± SD. **C**, Effect of recombinant Fibstatin on non-endothelial cell proliferation. One μg/ml of recombinant Fibstatin was applied to B16F10 or NIH-3T3 cells, stimulated with 1 ng/ml of FGF-2. No significant inhibition of proliferation was observed at day 5.

Fig. 4 : Fibstatin inhibits endothelial cells migration and tubulogenesis

A, Fibstatin effect on endothelial cell migration, tested in an *in vitro* wounding assay. Serum starved cells were stimulated with 3 ng/ml FGF-2 in the presence or not (control) of 1 μg/ml Fibstatin. After 14h, quantification of migrating cells into the wound area was determined under an inverted microscope. The data shown are the mean of a representative duplicate experiment. **B**, Tubulogenesis assay. ABAE cells were plated on Matrigel™ coated wells in the presence or not of 0.5 ng/ml FGF-2 with or without 1 μg/ml Fibstatin during 12 hours. Tube formation was quantified

with a Leica Q Win system. The data shown are the mean of a representative duplicate experiment.

Fig. 5: Fibstatin inhibits angiogenesis and tumor growth *in vivo*

A, Angiogenesis assay in Matrigel. Quantification of endothelial cells from Matrigel plugs injected subcutaneously in C57Bl6 mice, with FGF-2 alone (control), or in the presence of Fibstatin (Fib) or Endostatin (Endo). FGF-2 induced angiogenesis was significantly inhibited by Fibstatin compared to Endostatin. Data are expressed as percentage ± SEM, of the cell number obtained with FGF-2 alone, normalized (norm) (left) or not (right) with respect to the weight of the matrigel plug. Each experimental group contained 5 mice and the experiment was repeated twice with similar results. *P<0.05 was considered as statistically significant by using a one factor ANOVA.

B, Inhibition of B16F10 melanoma growth following gene electrotransfer of Fibstatin or Endostatin. C57Bl6 mice were inoculated subcutaneously with a suspension of B16F10 cells. Just after inoculation, therapy by electrotransfer was initiated. Each experimental group contained 15 animals. Each data represent the average tumor mass (± SEM) evaluated 10 days after the B16F10 inoculation. The difference between the Fibstatin and the control group were statistically significant. *P<0.05 was considered as statistically significant by using a one factor ANOVA. **C**, Reporter gene (LacZ) activity following electrotransfer into quadriceps. 10 days after the first electroporation, quadriceps were excised and β-galactosidase activity was determined in tissue homogenates using suitable commercial kit Galacto Light ™ (Tropix). Bars show the average β-galactosidase activity ± SD per 1 mg of muscle from 15 mice.

D, Endostatin concentrations in serum following electroporation of plasmid DNA containing or not (control) Endostatin gene, into quadriceps. Serum concentration of

Endostatin was measured 10 days after the first injection using a commercial kit (Accucyte Murine Endostatin Immunoassay Kit; Cytimmune Science). Each group contained 8 animals.

Fig. 6: Effect of Fibstatin gene delivery on tumor angiogenesis

A, Representative histological tumor sections were stained with an anti-mouse CD31. The immunostaining shows the rarefication of tumor blood vessels in Fibstatin and Endostatin-treated mice as compared to control mice. **B**, Quantitative analysis of CD31 immunostaining. The number of CD31 stained blood vessels was obtained from 10 different microscopic fields (magnification x200) from at least 5 different tumor sections. The data is represented as mean ± SD.

Fig 1

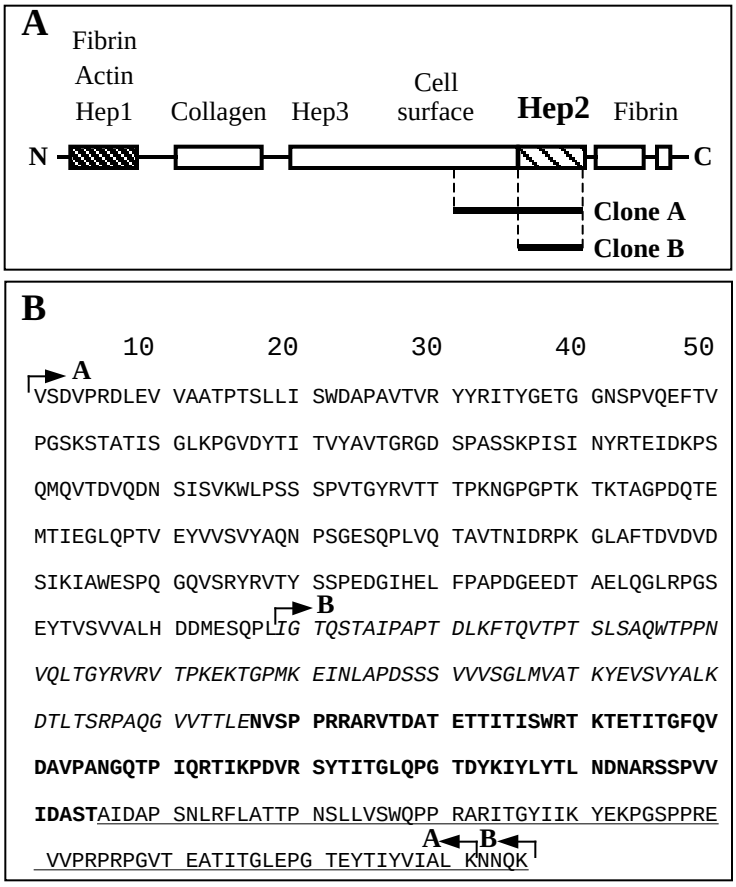
A
Fibrin
Actin
Hep1
Collagen
Hep3
Cell
surface
Hep2
Fibrin
N
C
Clone A
Clone B
B
10
20
30
40
50
A
VSDVPRDLEV VAATPTSLLI SWDAPAVTVR YYRITYGETG GNSPVQEFTV
PGSKSTATIS GLKPGVDYTI TVYAVTGRGD SPASSKPISI NYRTEIDKPS
QMQVTDVQDN SISVKWLPSS SPVTGYRVTT TPKNGPGPTK TKTAGPDQTE
MTIEGLQPTV EYVVSVYAQN PSGESQPLVQ TAVTNIDRPK GLAFTDVDVD
SIKIAWESPQ GQVSRYRVTY SSPEDGIHEL FPAPDGEEDT AELQGLRPGS
B
EYTVSVVALH DDMESQPLIG TQSTAIPAPT DLKFTQVTPT SLSAQWTPPN
VQLTGYRVRV TPKEKTGPMK EINLAPDSSS VVVSGLMVAT KYEVSVYALK
DTLTSRPAQG VVTTLENVSP PRRARVTDAT ETTITISWRT KTETITGFQV
DAVPANGQTP IQRTIKPDVR SYTITGLQPG TDYKIYLYTL NDNARSSPVV
IDASTAIDAP SNLRFLATTP NSLLVSWQPP RARITGYIIK YEKPGSPPRE
A
B
VVPRPRPGVT EATITGLEPG TEYTIYVIAL KNNQK

Fig 2

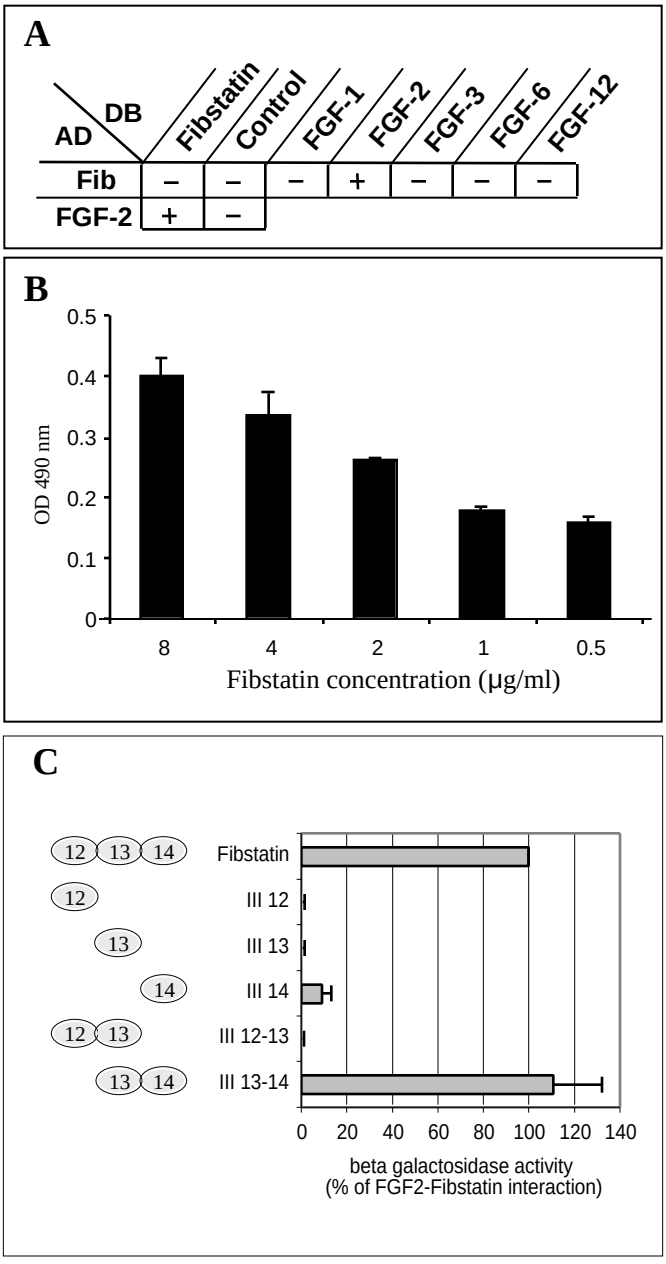
A
DB
AD
Fibstatin
Control
FGF-1
FGF-2
FGF-3
FGF-6
FGF-12
Fib
FGF-2
B
OD 490 nm
0.5
0.4
0.3
0.2
0.1
0
8
4
2
1
0.5
Fibstatin concentration (µg/ml)
C
12
13
14
Fibstatin
III 12
III 13
III 14
III 12-13
III 13-14
0
20
40
60
80
100
120
140
beta galactosidase activity
(% of FGF2-Fibstatin interaction)

Fig 3

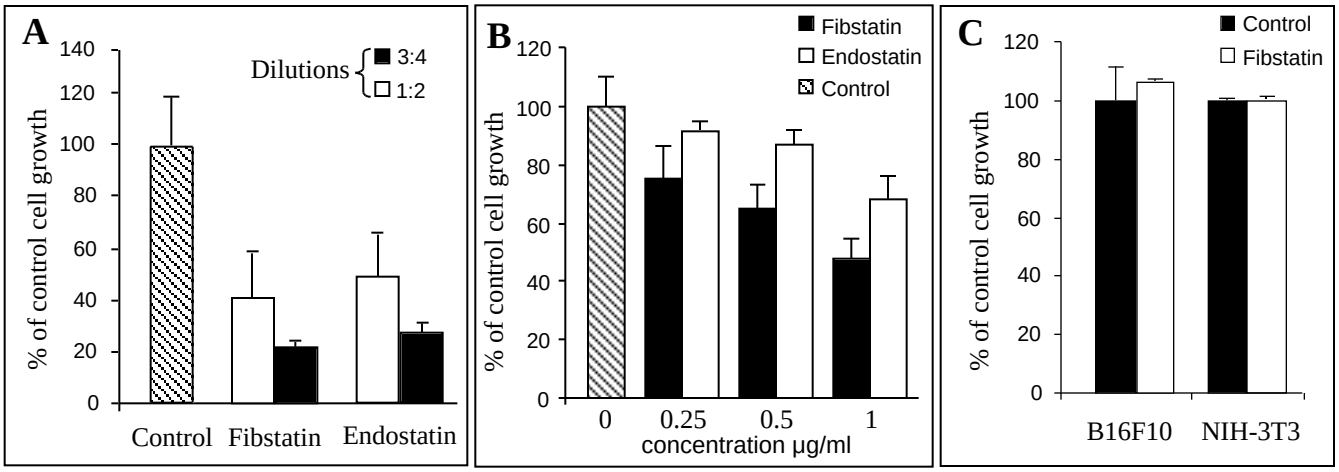
A
% of control cell growth
140
120
100
80
60
40
20
0
Dilutions
3:4
1:2
Control
Fibstatin
Endostatin
B
% of control cell growth
120
100
80
60
40
20
0
Fibstatin
Endostatin
Control
0
0.25
0.5
1
concentration µg/ml
C
% of control cell growth
120
100
80
60
40
20
0
Control
Fibstatin
B16F10
NIH-3T3

Fig 4

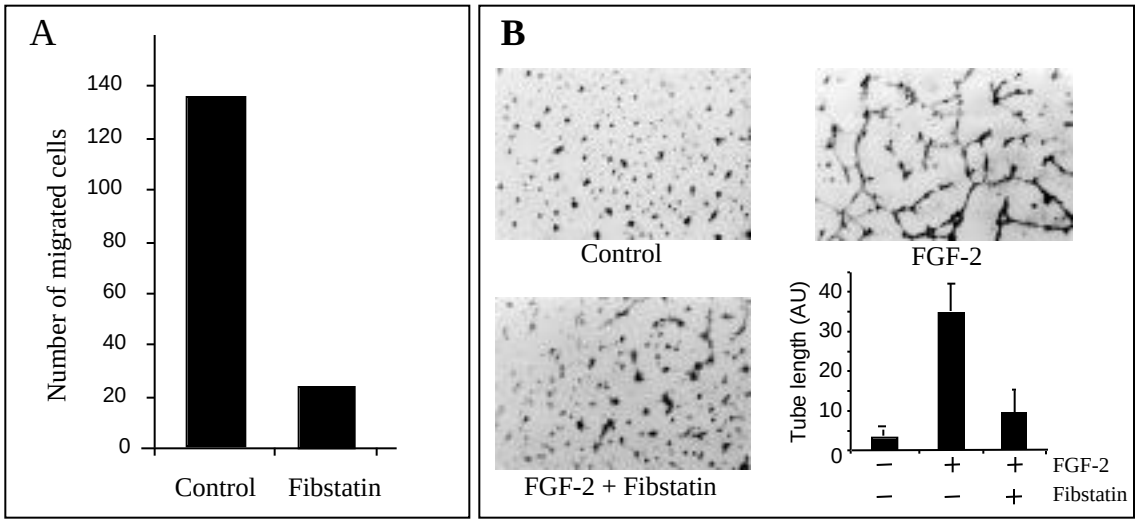
A
Number of migrated cells
140
120
100
80
60
40
20
0
Control
Fibstatin
B
Control
FGF-2
FGF-2 + Fibstatin
Tube length (AU)
40
30
20
10
0
–
+
+
FGF-2
–
–
+
Fibstatin

Fig 5

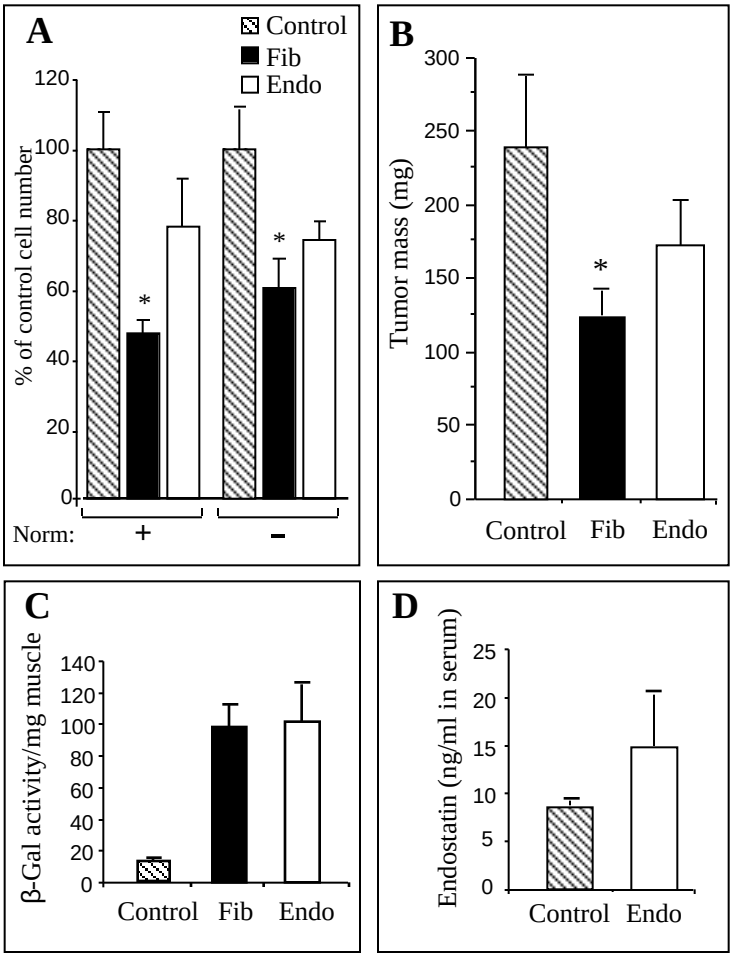
A
Control
Fib
Endo
% of control cell number
120
100
80
60
40
20
0
*
*
Norm:
+
–
B
Tumor mass (mg)
300
250
200
150
100
50
0
*
Control
Fib
Endo
C
β-Gal activity/mg muscle
140
120
100
80
60
40
20
0
Control
Fib
Endo
D
Endostatin (ng/ml in serum)
25
20
15
10
5
0
Control
Endo

Fig 6

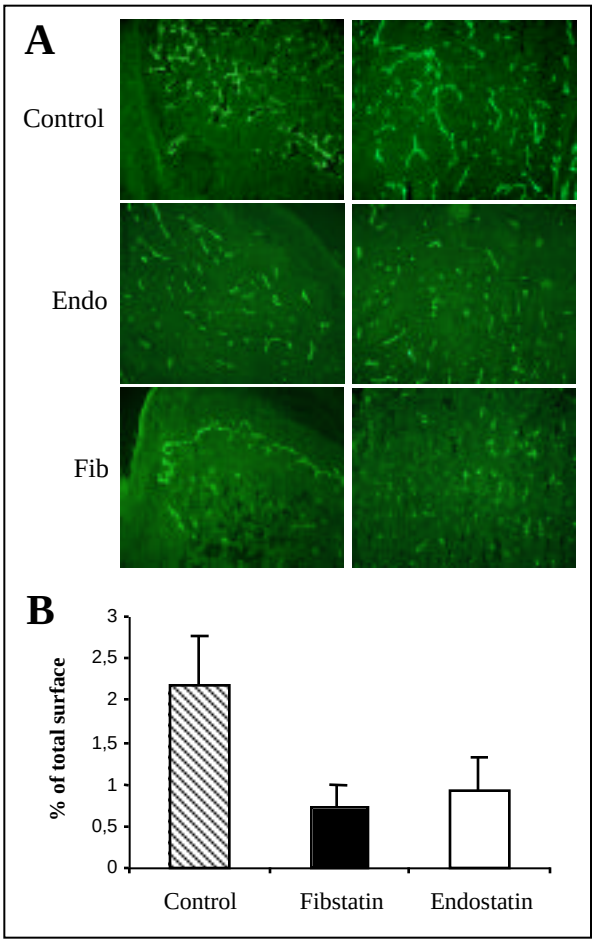
A
Control
Endo
Fib
B
% of total surface
3
2,5
2
1,5
1
0,5
0
Control
Fibstatin
Endostatin